ELSEVIER

Journal of Power Sources 68 (1997) 271–276

JOURNAL OF POWER SOURCES

Unique charge/discharge properties of carbon materials with different structures

Y.B. Roh [a,*], K.M. Jeong [a], H.G. Cho [a], H.Y. Kang [a], Y.S. Lee [b], S.K. Ryu [b], B.S. Lee [b]

[a] *Energy R&D Center, Samsung Display Devices Co., Ltd., 575, Shin-Dong, Paldal-Gu, Suwon City, Kyungki-Do 44-390, South Korea*

[b] *Department of Chemical Engineering, Chungnam National University, Taejon 305-764, South Korea*

Accepted 17 October 1996

Abstract

The electrochemical properties of isotropic and anisotropic carbon fibers were studied using the two-electrode method in a 1 M $LiPF_6$ electrolyte solution dissolved in a 1:1 volume mixture of ethylene carbonate (EC) and dimethyl carbonate (DMC). Isotropic carbon fiber had a larger irreversible capacity than that of the other carbon fibers and might have many sites for the electrolyte decompositon and residual lithium ions. Active carbon fibers prepared from isotropic carbon fibers by steam gasiformation at 850 °C showed large specific surface areas. After steam gasiformation, the active carbon fibers changed into a more crystalline state and had electrochemical characteritics similar to the anisotropic carbon fibers. Impedance profiles of the carbon fibers were fitted by equivalent analogs of a three-resistance–capacitance (RC) circuit in series and the thickness of passivation layers in the carbon fibers was calculated. © 1997 Published by Elsevier Science S.A.

Keywords. Carbon fibers; Voltage profile; Cyclic voltammogram; Alternating current impedance

1. Introduction

Carbon and graphite have been extensively studied as the anode materials in Li-ion batteries for attaining high capacity, long cycle life and safety [1]. The Li-ion insertion/desertion mechanism of carbon materials during charge and discharge, however, has not been understood clearly although several mechanisms have been proposed [2–4].

Pitch-based carbon fibers have been proposed as a promising anode material, because of various cross-sectional textures, showing excellent current rate capability and a rapid diffusion rate of the lithium ion in the carbon fiber during charge and discharge [1]. Anisotropic pitch-based mesophase structure, which has a semi-fluid state but containing crystallites to some extent, is easily graphitized by heat treatment. Isotropic pitch with a more amorphous and cross-linked structure than that of anisotropic pitch is difficult to graphitize at any heat-treatment temperature. Therefore, a study of the electrochemical properties of carbon fibers which are pyrolyzed from various kinds of pitch with different microstructures will contribute in the understanding of the insertion/desertion mechanism of the lithium ion and battery performance during charge and discharge.

In this study, we present electrochemical characteristics of carbon fibers such as voltage profile, cyclic voltammogram and impedance variation in order to elucidate insertion/extraction mechanism of lithium ions.

2. Experimental

Anisotropic round carbon fiber (ARCF) are prepared from coal tar and isotropic round carbon fiber (IRCF) from

Table 1
The properties of spinnable pitch [a]

Properties		Pitch	
		Isotropic	Anisotropic
Softening point		260	285
Solubility	QI (wt.%)	0.6	45.0
	BI (wt.%)	40	95.2
	HI (wt.%)	94	
OA (%)			99–100
After heat treatment process			
d_{002}			3.53
Specific surface area (m^2/g)		IRCF = 18, ACF = 1600	ACRF = 20

[a] QI: quinoline insoluble; BI: benzene insoluble; HI: hexane insoluble, and OA: optical anisotropic.

* Corresponding author.

0378-7753/97/$17.00 © 1997 Published by Elsevier Science S.A. All rights reserved
PII S0378-7753(96)02628-6

Naphtha Cracking Bottom Oil by nitrogen pressure spinning at 280 °C through a nozzle with a round opening and then undergoing stabilization by surface oxidation at 300 °C followed by carbonizing at 1000 °C. Table 1 shows the properties of spinnable isotropic and anisotropic pitches and X-ray results after carbonizing. Active carbon fiber (ACF) was also prepared by activating IRCF further in a steam gasiformation reaction at 850 °C.

Redox reactions of these carbon fibers were tested by a two-electrode system, i.e., stainless-steel coin cells (2016 type) in a dry box. The working electrodes contained one of the fibers: IRCF or ARCF or ACF, 5 wt.% (polytetrafluoroethylene) PTFE binder and 5 wt.% acetylene black. The counter electrode was a lithium metal foil. The electrolyte was 1 M $LiPF_6$ solution dissolved in a 1:1 volume mixture of ethylene carbonate (EC) and dimethyl carbonate (DMC).

Discharging and charging cycles were carried out between 0 and 3 V versus Li/Li^+ at a current density of 20 mA/g. Cyclic voltammograms of the carbon fiber electrodes were obtained at a scan rate of 0.05 mV/s with the ZANNER IM-6 system. The a.c. impedances were studied at open-circuit condition after having passed the electrical charge.

3. Results and discussion

Fig. 1 shows the voltage profiles of the first and second discharge (Li-ion insertion) and charge (lithium extraction)

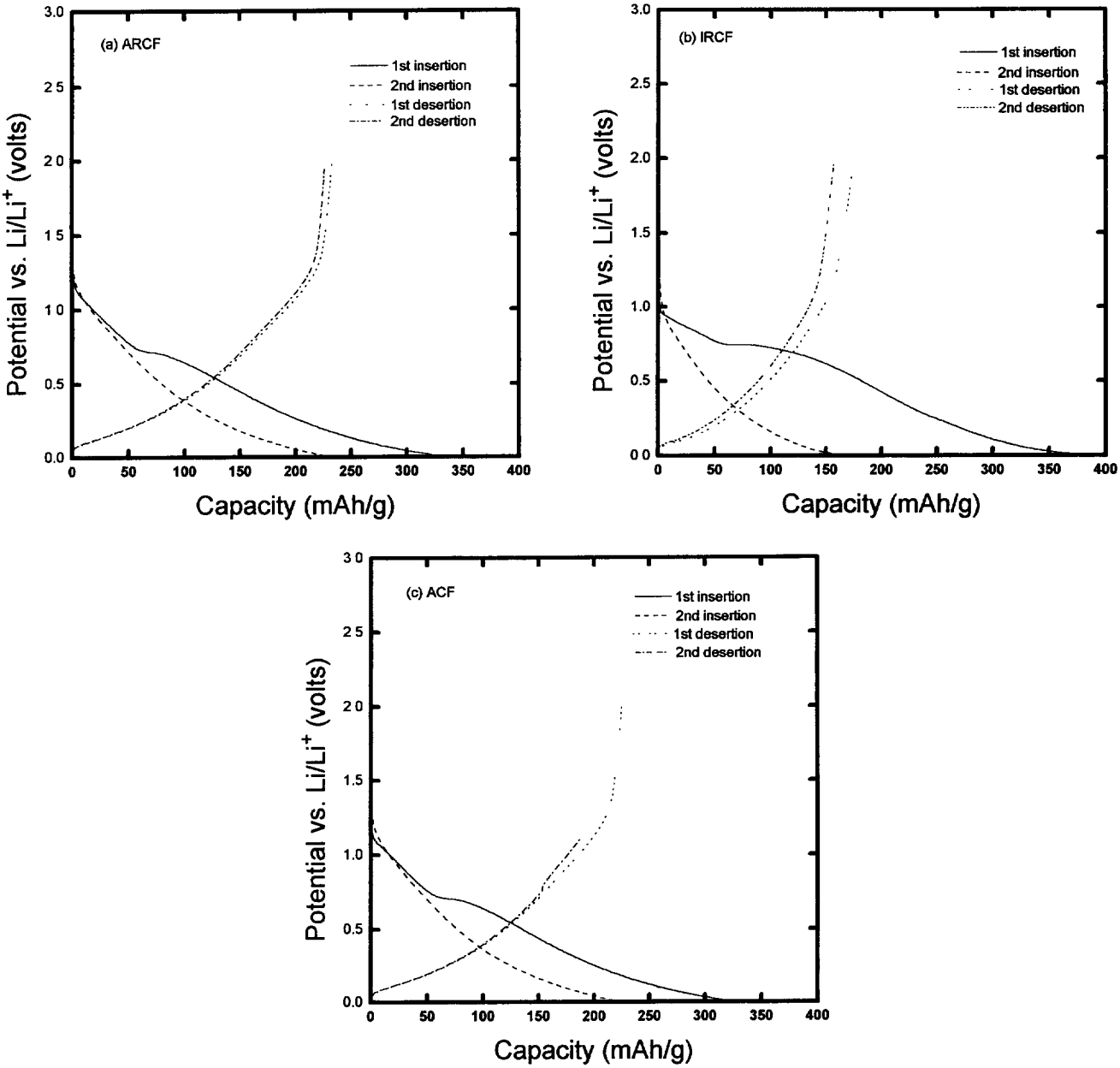

Fig. 1. Voltage profiles during the first and second discharge and charge in (a) ARCF, (b) IRCF and (c) ACF, current density: 20 mA/g.

of ARCF, IRCF and ACF at 20 mA/g current density. The potential curves for these carbon fibers at the first discharge are decreasing monotonously with increasing amount of lithium-ion insertion after showing the potential plateaus at 0.8 to 0.6 V versus Li/Li^+. These plateaus disappear at the second discharge.

The inclined voltage profiles during charging seem to indicate a uniform extraction reaction of the lithium ion. The irreversible capacity of IRCF for the first cycle is much larger than those of ARCF and ACF, see Fig. 1. The specific surface area of ACF, listed in Table 1, is much larger than that of ARCF and IRCF. On the contrary, it seems that the irreversible capacity of IRCF is not originated from the specific surface area [5].

The first-cycle irreversible capacity of carbon fibers may be caused not only by the electrolyte decomposition but also by the existence of the residual lithium ion in carbon fibers which does not take part in the reversible transfer of lithium ions during subsequent discharge and charge [8]. A similar amount of reversible capacity of ARCF and ACF with different surface areas indicates that the portion of the reversible capacity caused by the adsorption and desorption at the carbon surface is negligible.

Fig. 2 shows cyclic voltammograms of ARCF, IRCF and ACF, respectively. The potential was scanned from 1.5 V versus Li/Li^+ to the negative direction during the first and second discharge cycles with a scan rate of 0.05 mV/s. The ARCF and ACF fibers show a current plateau at about 1 V

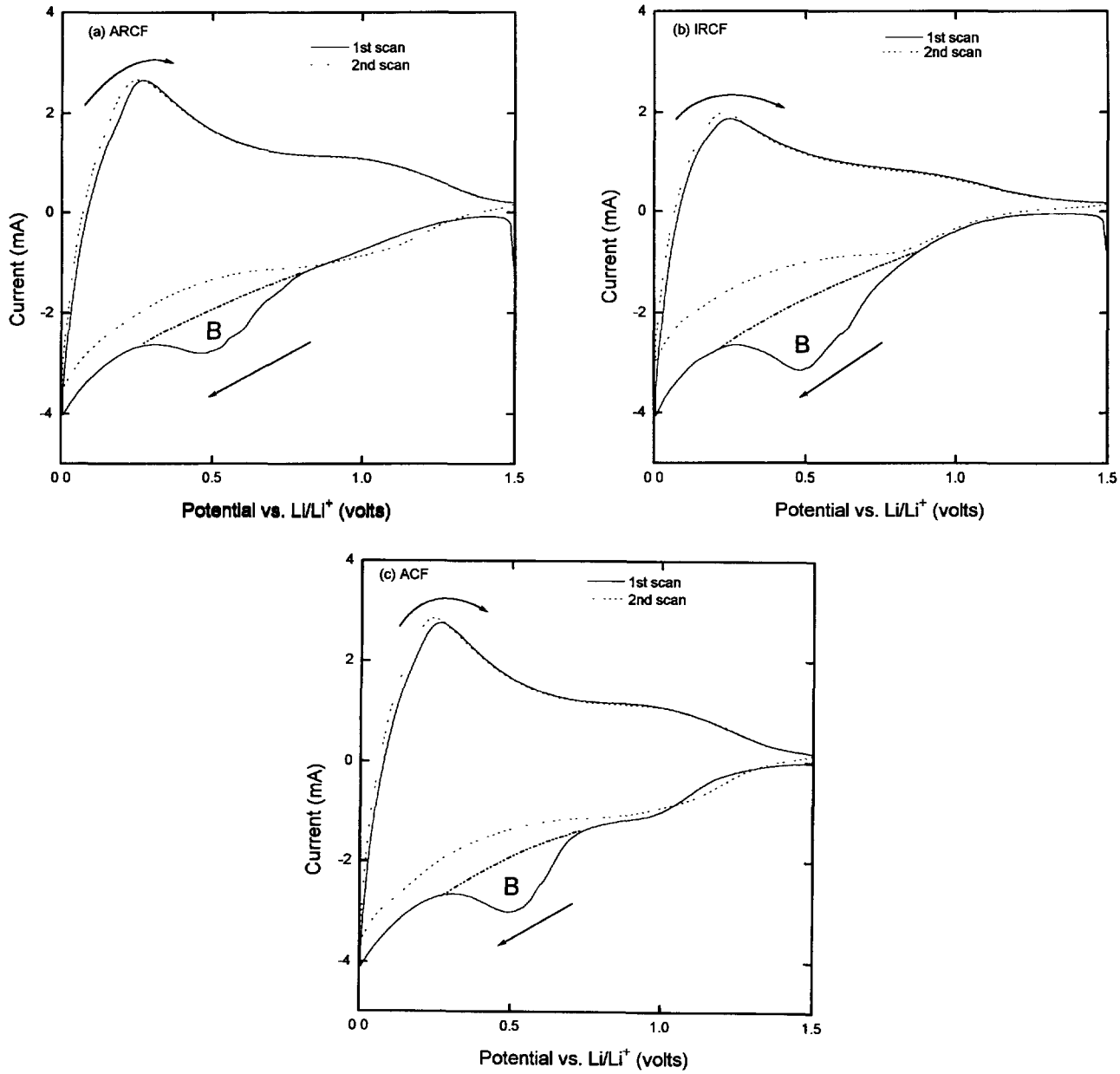

Fig. 2 Cyclic voltammograms of (a) ARCF, (b) IRCF and (c) ACF; scan rate: 0.05 mV/s.

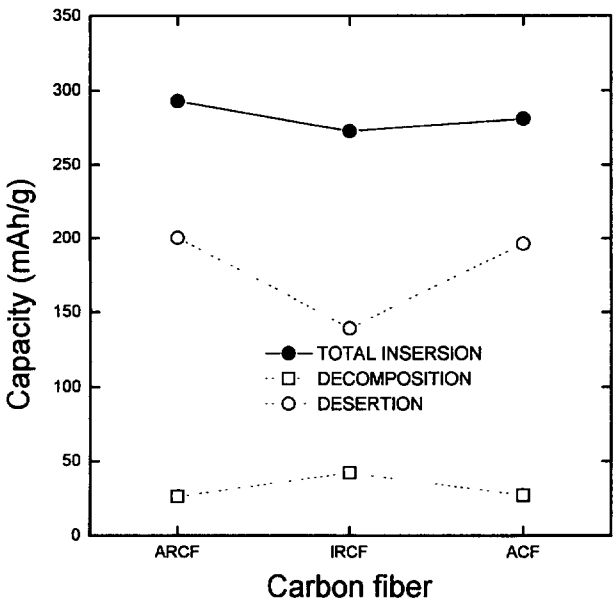

Fig. 3. Fractions of capacity composed of electrolyte decomposition and residual lithium ion during the first cycle.

and IRCF does not show any plateau during the first discharge. Nevertheless, the current peak at about 0.5 V can be seen in all carbon fibers. But the current peak at about 0.5 V is not found during the second cycle in the three carbon fibers. This current peak at 0.5 V during the first cycle is probably due to the formation of a passivation film caused by decomposition of the electrolyte. The cyclic voltammetry behavior caused by electrolyte decomposition, which is thought to take place at a definite potential range, can be described by region B (Fig. 2) of the voltammograms for the three carbon fibers. However, the behavior due to the residual lithium ions during the first cycle, which is thought to take place at various potential sites in carbon, increased monotonously with decreasing potential as indicated by the dotted line. Therefore, the amount of irreversible capacity caused by the residual lithium ions during the first cycle can be obtained by subtracting from the cathodic charge passed to the fraction of capacity due to the electrolyte decomposition (B) and the sum of the anodic charge passed.

Fig. 3 shows each fraction of capacity which is composed of electrolyte decomposition and residual lithium ion during the first cycle. As obvious from Fig. 3, the amount of residual

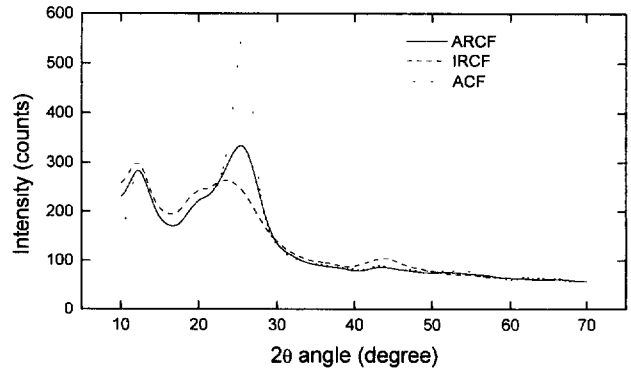

Fig. 4. XRD profiles of ARCF, IRCF and ACF

lithium ion is much larger than that of the electrolyte decomposition in all the carbon fibers. IRCF has much larger irreversible capacity, compared with that of ARCF and ACF. It means that IRCF pyrolyzed from pitch with an isotropic structure has many sites for electrolyte decompositon and residual lithium-ion storage in carbon. However, ACF activated from the same isotropic pitch showed a markedly different behavior due to the structural change through the activation process such as steam gasfication as shown in Fig. 4.

Fig. 5 shows typical Cole–Cole plots after the first cycle in the frequency range from 1 MHz to 10 mHz. The a.c. impedance was measured at open-circuit potential of about 1 V for each discharged carbon fiber. In Fig. 5, the apparent differences between ARCF, ACF and IRCF could be found easily.

The impedance of the two film-covered carbon fiber/electrolyte interfaces should be modeled by a three-RC circuit with an electrolyte resistance as shown in Fig. 6. All values of resistance and capacitance have been calculated and are listed in Table 2. The high frequency region is mainly affected by the electrolyte and passivation layer formed on the carbon fiber surface. The medium frequency region shows the resistance of charge transfer and the double-layer capacitance. The low frequency region shows a straight line, implying that the system is controlled by lithium-ion diffusion in the carbon fiber [6].

$R_{film,c}$ (resistance of compact passivation film) and $R_{film,p}$ (resistance of porous passivation film) values of the high frequency region in IRCF are much larger than those of other carbon fibers and the two regions of high and medium fre-

Table 2
The value of estimated impedance

	R_e (Ω cm)	R_{ct} (Ω cm)	C_{dl} (mF/cm^2)	$R_{film,c}$ (Ω cm)	$C_{film,c}$ (μF/cm^2)	$R_{film,p}$ (Ω cm)	$C_{film,p}$ (μF/cm^2)	$t_{film,c}$ (Å)	$t_{film,p}$ (Å)
ARCF	281	561	0.90	149	1.63	389	22 13	27	2
IRCF	368	1035	0.90	298	0 67	806	11.33	67	3.9
ACF	204	642	0.43	138	1 55	507	13.85	21	3.2

R_{ct} = charge-transfer resistance, $R_{film,c}$ = resistance of compact passivation film, $R_{film,p}$ = resistance of porous passivation film, R_e = electrolyte resistance, $t_{film,c}$ = thickness of compact passivation film, C_{dl} = double-layer capacitance, $C_{film,c}$ = capacitance of compact passivation film, $C_{film,p}$ = capacitance of porous passivation film, $t_{film,p}$ = thickness of porous passivation film.

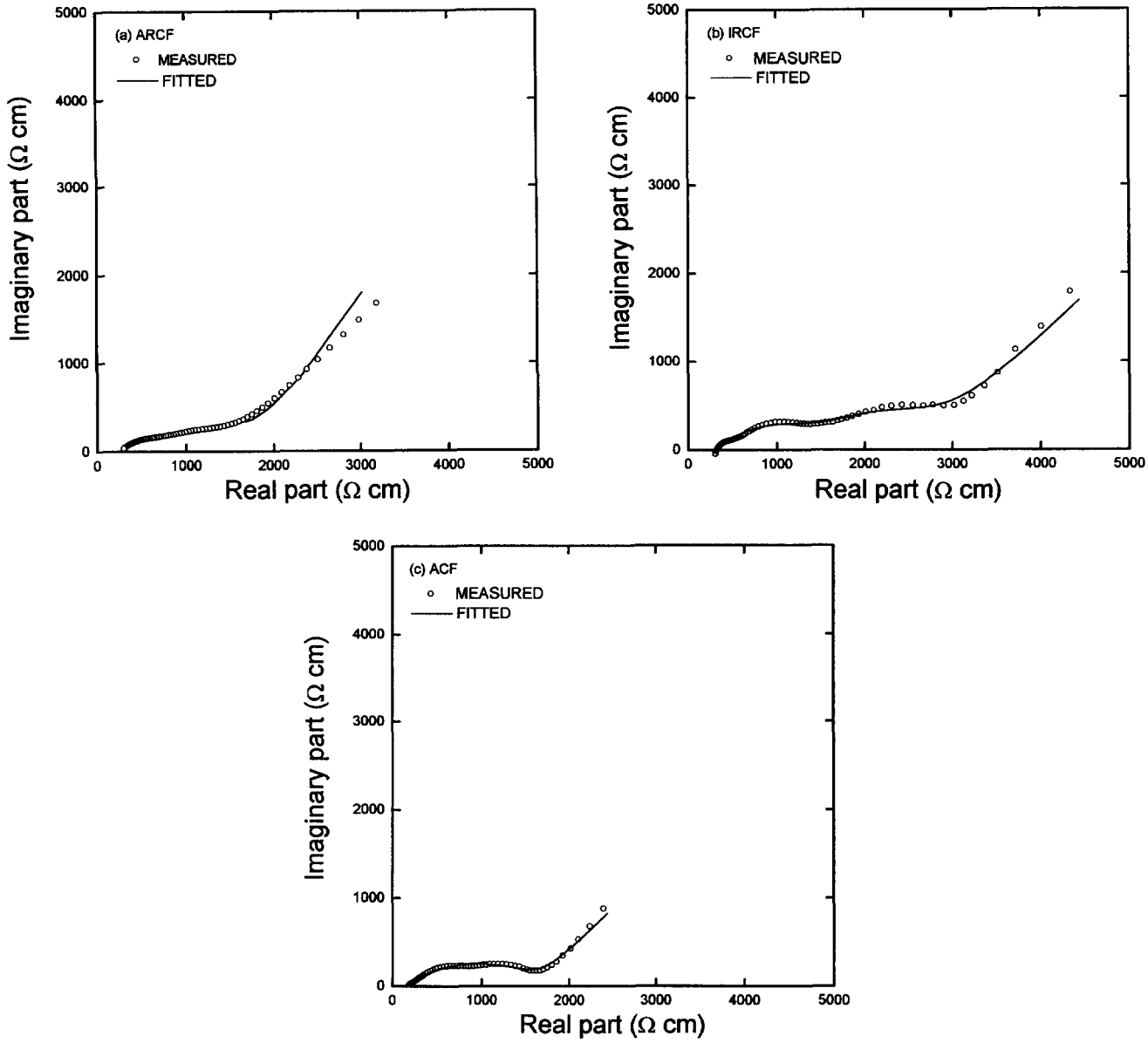

Fig 5 Cole–Cole plots after the first cycle in the frequency range from 1 MHz to 10 mHz for the discharged fibers: (a) ARCF, (b(IRCF, and (c) ACF.

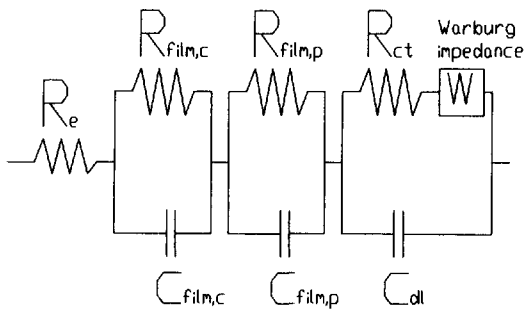

Fig. 6. Equivalent circuit models for two film-covered carbon fiber/electrolyte interfaces: R_{ct}: charge-transfer resistance; C_{dl}: double-layer capacitance, $R_{film,c}$ resistance of the compact passivation film; $C_{film,c}$: capacitance of the compact passivation film; $R_{film,p}$. resistance of the porous passivation film, $C_{film,c}$ capacitance of the us passivation film, and R_e: electrolyte resistance

quency are split more clearly. As listed in Table 2, R_e (resistance of electrolyte) is almost constant at all carbon fibers but $R_{film,c}$, $R_{film,p}$ and R_{ct}(charge-transfer resistance) are the largest in IRCF. It means that the passivation film deposited is much thicker on IRCF and that the charge-transfer rate of IRCF is also slower than those of ARCF and ACF. The thickness of each passivation

$$t_{film} = \epsilon_0 \frac{KA}{C_{film}} \quad (1)$$

film, assuming two layer composed of a compact and porous plated geometry, can be calculated using Eq. (1) where t_{film} is the thickness of the compact or porous passivation film, ϵ_0 the dielectric constant of the vacuum, K the dielectric constant

of the each passivation film, and A the electrode area. The dielectric constant of the passivation film assumed about to be 5 (corresponding to the dielectric constant of Li_2CO_3, LiF and LiOH [7]). Thickness values of the passivation layer at each carbon fiber are listed in Table 2, assuming a roughness factor of 1 [7]. This value almost agrees with that published by Fong et al. [5]. IRCF has a thicker passivation film than the other carbon fibers, which means that its irreversible capacity is larger.

The formation mechanism of the passivation film on the carbon fiber surface has not been examined clearly although several formation mechanisms were proposed so far and are needed to be clarified in the near future.

4. Conclusions

The characteristic electrochemical properties of various carbon fibers have been studied and the experimental results are as follows.

1. The irreversible capacity of each of the carbon fibers might be caused not only by the electrolyte decomposition but also by the existence of residual lithium ions in carbon during the first cycle. The amount of irreversible residual lithium ion was much larger than that of electrolyte decompositon at all of carbon fibers.

2. IRCF had a much larger irreversible capacity than that of the other carbon fibers and might have many sites for the electrolyte decompositon and residual lithium ions.

3. ACF prepared by steam gasiformation at 850 °C showed a large specific surface area. After steam gasiformation, ACF changed into a more crystalline state. The electrochemical characteristics of ACF was similar to that of ARCF.

4. The impedance profiles of carbon fibers were fitted by equivalent analogs of a three-RC circuit in series; the thicknesses of the compact and porous passivation films in carbon fibers were calculated.

References

[1] N. Takami, A. Satoh, M. Hara and T. Ohsaki, *J. Electrochem Soc., 142* (1995) 2564.
[2] A. Mabuchi and K. Tokumitsu, *J. Electrochem Soc., 142* (1995) 1041.
[3] K. Sato, M. Noguchi, A. Demachi, N. Oki and M. Endo, *Science, 264* (1994) 556.
[4] J.R. Dahn, T. Zheng, Y. Liu and J.S Xue, *Science, 270* (1995) 590.
[5] R Fong, U. von Sacken and J.R Dahn, *J. Electrochem. Soc., 137* (1990) 2009.
[6] M Morita, N. Nishimura and Y. Matsuda, *Electrochim Acta, 38* (1993) 1721.
[7] D. Aurbach, A Zaban et al., *J. Electrochem. Soc., 142* (1995) 2873.
[8] Y. Matsumura, S. Wang and J. Mondori, *J. Electrochem Soc., 142* (1995) 2914.